

M. Plasilova¹, C. Chattopadhyay^{2,3}, P. Pal^{2,4}, A. Ghosh², K. Heinemann¹

¹ Research Group Human Genetics, Division of Medical Genetics UKBB, Center of Biomedicine DKBB

² University Children's Hospital, University of Basel, Switzerland, ²Institute of Child Health, Calcutta, India

³ Calcutta Project Foundation, University of Basel, Switzerland, ⁴S.B. Devi Charity Home, Calcutta, India



Introduction

Hutchinson-Gilford progeria syndrome (HGPS) is an extremely rare genetic disorder with children displaying features reminiscent of premature senescence. Recurrent heterozygous de novo point mutations in the *LMNA* gene encoding lamin A/C, a component of the filamentous meshwork of the nuclear lamina, have been shown to cause sporadic, non-familial HGPS. Recently, we have provided molecular evidence for autosomal recessive inheritance of HGPS in a consanguineous Indian family (Figure 3E). In this family all 4 affected children carry the homozygous missense mutation c.1626G>C (p.Lys542Asn; K542N), whereas their parents as well as a sister are healthy heterozygous mutation carriers.

To assess the pathogenic consequences of the K542N mutation, we investigated primary cultured skin fibroblasts from affected homozygous and healthy heterozygous mutation carriers for a) morphological changes in the nuclear envelope, b) telomere length alterations, and c) differences in gene expression using GeneChip® Human Genome U133 Plus 2.0 2 arrays. Here we present initial results on the molecular pathogenesis of the K542N *LMNA* mutation.

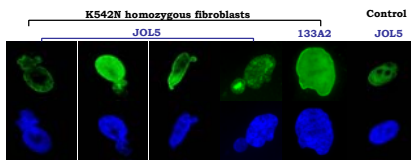


Figure 1 An irregular shape of the nuclear envelope and envelope interruptions accompanied by chromatin extrusion in the primary cultured fibroblast from homozygous carriers of K542N

Table 1 The average frequency of lobulated nuclei in the primary cultured fibroblasts

<i>LMNA</i> genotype	133A2 immunofluorescence	JOL5 immunofluorescence
K542N homozygotes (n=3)	21.2%	13.4%
K542N heterozygotes (n=3)	3.9%	2.9%
Wild-type controls (n=2)	0.7%	1.6%

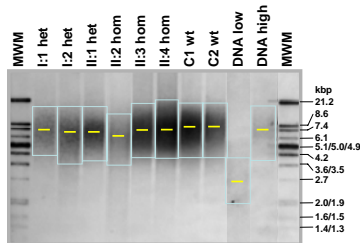


Figure 2 Southern analysis of terminal restriction fragments (TRF) on blood extracted DNA. Blue bars indicate range of the TRF length for each sample; yellow line - median TRF length; wt - wild type *LMNA*, het and hom - heterozygous and homozygous carrier of K542N, respectively; family members are numbered as indicated in pedigree (Figure 3E); C1, C2 - controls; "DNA low" and "DNA high" - control DNA with low and high molecular weight telomeres, respectively (TeloTAGGG Telomere Length Assay, Roche)

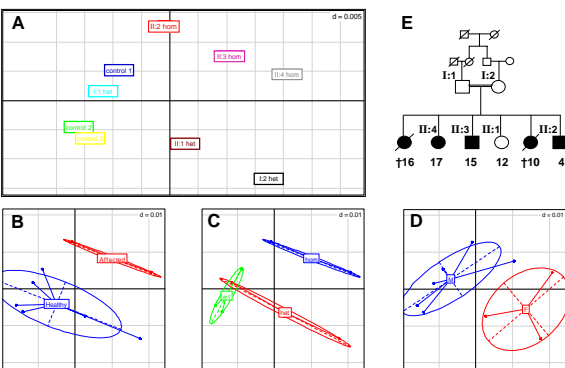


Figure 3 Between group analysis (BGA). A) scatterplot of the microarray samples, showing their separation on the discriminating BGA axes (wt - wild type *LMNA*; het - heterozygous carrier of K542N; hom - homozygous carrier of K542N). B) projection of the samples according to the phenotype, C) according to the mutation status, and D) according to the gender (M - male; F - female). E) HGPS pedigree (number under bars indicates age at skin biopsy or age at death)

Material

Primary skin fibroblast cultures were established from a skin biopsy of 3 healthy male *LMNA* wild-type controls, 3 unaffected heterozygotes and 3 affected homozygotes K542N *LMNA* mutation carriers (written informed consent, for this study has been obtained from all family members and healthy controls). Cells were cultured in Minimal Essential Medium (MEM; BioConcept) supplemented with 20% foetal calf bovine serum and 0.1% gentamycin (Sigma-Aldrich). When fibroblasts reached 60-70% confluence, they were used either for DNA or total RNA extraction, according to the manufacturer's protocols (DNeasy Blood & Tissue Kit and RNeasy Mini kit, respectively; QIAGEN).

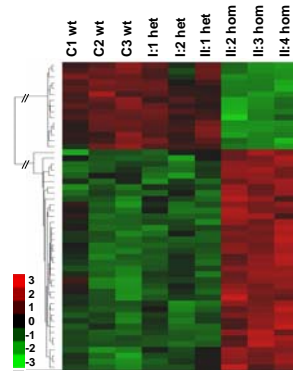


Figure 4 Hierarchical cluster analysis of the differentially expressed genes. wt - indicates wild type *LMNA*, het and hom - heterozygous and homozygous carrier of K542N, respectively; C1, C2, C3 - controls; family members are numbered as indicated in pedigree (Figure 3E). Colour bar shows the level of gene expression change: red indicates over-expression, green indicates under-expression, and black indicates no change; intensity of colour correlates to the magnitude of change.

Table 2 Over-represented biological processes associated with gene expression changes

GO ID	biological process	p	nr.obs	nr.array
GO:0007275	multicellular organismal development	1.16E-05	18	1586
GO:0009653	anatomical structure morphogenesis	4.58E-05	14	1090
GO:0009887	organ morphogenesis	0.000409	11	861
GO:0030154	cell differentiation	0.000511	7	361
GO:0048513	organ development	0.000658	11	910
GO:0007399	nervous system development	0.00086	7	394
GO:0007267	cell-cell signaling	0.003018	7	490
GO:0040007	growth	0.021728	3	149
GO:0050793	regulation of development	0.023679	3	154
GO:0031324	negative regulation of cellular metabolism	0.025723	3	159
GO:0051246	regulation of protein metabolism	0.02786	3	164
GO:0009892	negative regulation of metabolism	0.0394	3	188
GO:0042221	response to chemical substance	0.043162	3	195
GO:0009611	response to wounding	0.047074	4	341
GO:0044255	cellular lipid metabolism	0.050512	4	349

Note: GO ID - GO accession number; nr.array - indicates the number of genes that can be detected using GeneChip® Human Genome U133 Plus 2.0 2 arrays; nr.obs - the number of genes of interest that were mapped to the specific GO term

Results

Nuclear (envelope) morphometric analysis

Investigation of DAPI stained nuclei from primary cultured fibroblasts revealed increased frequency of the chromatin extrusion and irregularly shaped nuclei in patients when compared to healthy heterozygotes and wild-type controls (Table 1). Immunofluorescent staining using lamin A and lamin A/C specific antibodies (133A2 and JoL5, respectively) showed that these extrusions were accompanied by extensive interruptions of the nuclear envelope.

Telomere length analysis

No significant difference in telomere lengths was observed between affected homozygous and healthy heterozygous mutation carriers and/or wild-type controls when investigating DNA from blood and primary cultured fibroblasts (Student's t-test: $p=0.4189$; Figure 2).

Gene Expression profiling

To investigate gene expression changes caused by K542N/K542N *LMNA* mutation we compared the entire transcriptome of primary cultured fibroblasts from homozygous patients with that of heterozygous healthy family members, and wild-type controls by using GeneChip® Human Genome U133 Plus 2.0 2 arrays. Moderated t-statistics and between group analysis (BGA) of the whole set of genes were applied to identify genes which provide the best discrimination between patients and healthy individuals. Classification of the samples based on the differentially expressed genes is illustrated in Figure 3A-D. Top 100 genes discriminating affected individuals from that of healthy were selected and further subjected to Gene ontology (GO) classification. GO classification revealed that these top 100 genes are involved mainly in the development, organogenesis, morphogenesis, growth regulation, and cell differentiation (Table 2). Intriguingly, nuclear lamina associated genes, such as lamin A/C (*LMNA*), lamin B1 (*LMNB1*), lamin B2 (*LMNB2*), and emerin (*EMD*), showed no statistically significant expression differences between homozygotes, heterozygotes and wild-type controls ($p=0.38-0.77$). Result of a hierarchical cluster analysis of the top differentially expressed genes is shown in Figure 4.

Conclusions

Similar to observation in HGPS patients heterozygous for the de novo G608G splicing mutation, the K542N/K542N *LMNA* mutation is associated with significant changes in nuclear shape, i.e. nuclear envelope lobulation, extensive interruptions of the nuclear envelope, and chromatin extrusion.

No significant telomere shortening could be detected in blood leukocyte and primary skin fibroblasts of the K542N/K542N carriers.

Genome-wide gene expression analysis revealed that the K542N mutation leads to statistically significant altered expression of genes involved in development, organogenesis, differentiation, as well as more specifically in cellular lipid metabolism.

These results are currently being confirmed by complementary investigations (at the RNA and protein level) and should help to better understand the mechanisms leading to the extensive skeletal lesions and lipodystrophy in HGPS.

Methods

Immunofluorescence and nuclear morphometric analysis

Immunofluorescence was performed on the 3rd passage primary cultured skin fibroblasts. Mouse monoclonal antibodies 133A2 and JoL5 (Acris Antibodies) specific to lamin A and lamin A/C, respectively, were used at 1:100 and 1:10 dilution into 1xPBS with 1%BSA. Cells were fixed 10 min. in 2% PFA. Slides were counterstained with DAPI (Sigma-Aldrich) and mounted in Vectashield antifade solution (Vector Laboratories). To determine whether K542N mutation leads to irregular nuclear shapes, the overall percentage of lobulated or malformed nuclei was scored in 200 nuclei from each of 6 family members (3 K542N homozygotes and 3 heterozygotes) and 2 *LMNA* wild-type healthy controls. These examinations were performed in a double-blind count.

Telomere length assay

Telomere length was investigated on both blood and fibroblast extracted DNA from all 6 family members and 2 healthy controls. Southern analysis of terminal restriction fragments (TRF), obtained by digestion of genomic DNA using *HinfI* and *RsaI* restriction enzymes, was performed using TeloTAGGG Telomere Length Assay, according to the manufacturer's protocol (Roche, Switzerland). Differences of the TRF length between healthy and affected individuals were evaluated by Student's t-test.

Gene Expression profiling

Total RNA isolated from the primary skin fibroblasts was subjected to synthesis of double-stranded cDNA and biotin-labelled cRNA according to the manufacturer's protocol (Affymetrix). Fragmented cRNA preparations were hybridized to GeneChip® Human Genome U133 Plus 2.0 2 arrays (Affymetrix) and scanned on a GeneChip Scanner 3000 7G (Affymetrix). Pre-processing of Affymetrix GeneChip raw data was performed using Robust Multi-Array (RMA) normalization method, Bioconductor affy package. Statistically significant differentially expressed genes were detected by bayesian approach using moderated t-statistics from the Bioconductor limma package. In addition, classification and class prediction using between group analysis (BGA) of the whole set of gene dataset was performed by means of Bioconductor MADE4 package. Top 100 differentially expressed genes were further subjected to gene ontology (GO) classification. Threshold p-value of 0.05 was used to identify significantly over-represented GO-classified biological processes for the genes of interest. Hierarchical cluster analysis of the differentially expressed genes was performed according to Eisen et al., 1998 (PNAS 95: 14863-14868), applying median centering of genes, Pearson correlation coefficients as distance measures, and clustering over the genes.